

Determination of the coherence length and beat frequency length using a p-emf sensor

P. Rodríguez-Montero^a, A. S. Cruz-Félix^a, E. Tepichín-Rodríguez^a, A. F. Muñoz-Potosí^b, and L. G. Valdivieso-González^b

^a*Instituto Nacional de Astrofísica, Óptica y Electrónica,
Luis Enrique Erro # 1, Tonantzintla, Pue. 72840, México.*

^b*Grupo de Investigación GICBA, Unidades Tecnológicas de Santander,
Av. Los Estudiantes # 9-82, Bucaramanga, Santander 680003, Colombia.*

Received 21 August 2024; accepted 2 December 2024

The coherence of light is essential for understanding interference phenomena, which are pivotal in a wide range of applications. However, due to the technical challenges of conventional methods, quantifying coherence is difficult to achieve in undergraduate optics laboratories. In this work, we present a modification of a method and experimental setup that can enhance the understanding of coherence concepts employing a sensor based on the non-steady-state photo-electromotive force (p-emf) effect. This p-emf sensor generates an electrical current proportional to the square of the interference pattern's visibility, eliminating the need for image processing and high-quality optical elements, and allowing for real-time measurements. We demonstrated the method by measuring the coherence length of a He-Ne laser and the corresponding length associated with the beat frequency of the laser cavity's longitudinal modes. This approach is robust, straightforward and simple, making it suitable for implementation in undergraduate optics laboratories.

Keywords: Temporal coherence; coherence length; p-emf sensors; interferometry.

DOI: <https://doi.org/10.31349/RevMexFisE.22.020220>

1. Introduction

In a broad sense, coherence is the capacity of two light beams to interfere with each other. Coherence is usually categorized into spatial and temporal coherence. The visibility of the interference pattern measures the degree of coherence between the two interfering beams.

Understanding the temporal coherence of light is highly significant. Various methods have been reported for evaluating the temporal coherence, or equivalently, the coherence length of a light source. These include methods based on analyzing the modulations of the contrast and polarization state of the interference patterns [1], employing holographic optics [2], utilizing two-wave mixing in photorefractive crystals [3], and the widely adopted approach of using a Michelson interferometer [4,5].

In the methods employing the Michelson interferometer, the typical procedure for determining the coherence length of the light source involves assessing the visibility of the interference pattern as a function of the optical path difference. Visibility is evaluated by analyzing and applying specific criteria to the interference patterns captured with a CCD sensor. To ensure reliable results, several requirements must be met. These include setting up the interferometer on a vibration-isolated optical table, conducting the tests with the laboratory illumination lights turned off or placing optical band filters in front of the CCD sensor, adjusting the intensity of the interfering beams incident on the CCD, optimizing the gain and exposure time of the CCD, and carefully aligning the entire setup [5].

The aforementioned requirements are time-consuming and difficult to achieve in a typical student laboratory. In this

paper, we report a modification to a method that utilizes a p-emf sensor to measure the coherence length and the beat frequency length of longitudinal modes within the He-Ne laser cavity. As described below, this sensor generates in real time an electrical current proportional to the square of the interference pattern visibility [6]. Hence, utilizing this sensor allows us to detect gradual changes in the interference pattern visibility as a function of the optical path difference of the interfering beams. In contrast to the aforementioned methods, the proposed method does not require recording and processing the interference pattern, using high-quality optical elements, vibration isolation tables, or carrying on the experiment in a dark room. These features of the proposed method make it well-suited for implementation in an undergraduate optics laboratory.

1.1. Two beam interference

Consider an amplitude-splitting interferometer, such as the Michelson interferometer, in which two partially coherent plane wavefront beams of intensities I_1 and I_2 and wavelength λ interfere, forming an angle θ between them, as depicted in Fig. 1.

The intensity of the interference pattern is given by:

$$I(\Delta L, x) = I_0 \left[1 + V \cos \left(\frac{2\pi x}{p} + \phi(\Delta L) \right) \right], \quad (1)$$

where $I_0 = I_1 + I_2$ is the average irradiance of the interference pattern on the interference plane, ΔL is the optical path difference between the beams, $p \simeq \lambda/2\theta$ is the spatial period of the interference fringes for angles $\theta \ll 1$, and $\phi(\Delta L)$ is a

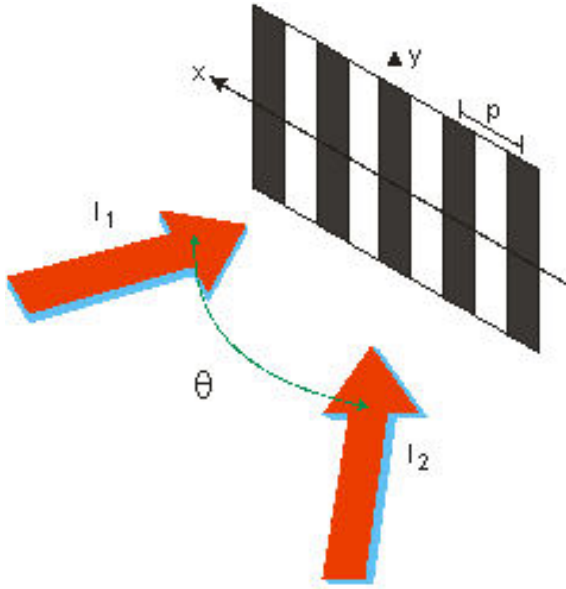


FIGURE 1. Interference of two mutually coherent plane wavefront beams. p stands for the period of the interference fringes.

phase that depends on ΔL . The visibility V of the interference pattern, which is given by [7]:

$$V = \frac{2\sqrt{I_1 I_2}}{I_0} |\gamma(\Delta L)|. \quad (2)$$

In this equation $\gamma(\Delta L)$ stands for the modulus of the complex degree of coherence. Hence, by measuring the visibility of the interference pattern as a function of the optical path difference, one can determine the modulus of the complex degree of coherence and the coherence length of the light source.

1.2. P-emf sensors

The p-emf sensors are based on the non-steady-state photoelectromotive force (p-emf) effect [6]. This effect consists in the generation of an alternating electrical current through a short-circuited photoconductive material when it is illuminated by a vibrating, spatially non-uniform light pattern. The electrical current is the result of the spatial mismatch between the relatively stable space-charge electric field distribution $E_{SC}(x)$ stored in the impurity centers of the photoconductive material and the photo-excited carriers' distribution, which follows the instantaneous light distribution $I(x, t)$.

A simple way to observe the p-emf effect is to illuminate the photoconductive sample with an interference pattern formed by two coherent plane waves, where one of the beams is phase-modulated at frequency f , causing the interference pattern to vibrate accordingly. For the purposes of this work the amplitude of the electrical current i_f generated by the p-emf sensor at frequency f as a function of the interference pattern visibility can be expressed as [8,9]:

$$i_f(V) = CAI_0V^2K(\theta)F(f). \quad (3)$$

In this equation, A is the amplitude of the phase modulation, $K(\theta)$ and $F(f)$ are functions that depend on the spatial frequency of the interference pattern and the phase modulation frequency, respectively. The constant C groups several electro-optical constants of the photoconductive sample.

These p-emf sensors can efficiently detect high-frequency, low-amplitude phase modulated signals even in the presence of low-frequency, high-amplitude phase shifts, such as those caused by environmental perturbations. They can also produce an efficient electrical signal with interfering beams that have irregular wavefronts, including those modulated with speckle. These capabilities result from the dynamic properties of the space charge electric field $E_{SC}(x)$ and the holographic processes involved in forming the p-emf electrical current [6,10]. These sensors have been employed for measuring the short coherence length of superluminescent diodes when one of the interfering beams is affected by speckle [11], characterization of femtosecond pulses [12], detecting laser-generated ultrasonic waves [10], and monitoring cardiac activity [13].

In this paper, we utilize the fact that the electrical current generated by p-emf sensors, or p-emf signals is proportional to the square of the visibility, while keeping the rest of the parameters constant:

$$i_f \propto V^2. \quad (4)$$

The p-emf sensor is similar to that reported in Ref. [9]. It was fabricated from a GaAs:Cr crystal with approximate dimensions of $3.2 \times 3.2 \times 0.5$ mm, attached to a printed circuit board. Two parallel electrodes were deposited on its front surface (3.2×3.2 mm) using silver paint, creating effective interelectrode dimensions of $L_x \cong 1.0$ mm (horizontal) and $L_y \cong 3.2$ mm (vertical). To extract the electrical current, the silver-painted electrodes were connected to a coaxial cable using short gold wires. A photograph of the employed p-emf sensor is shown in Fig. 2.

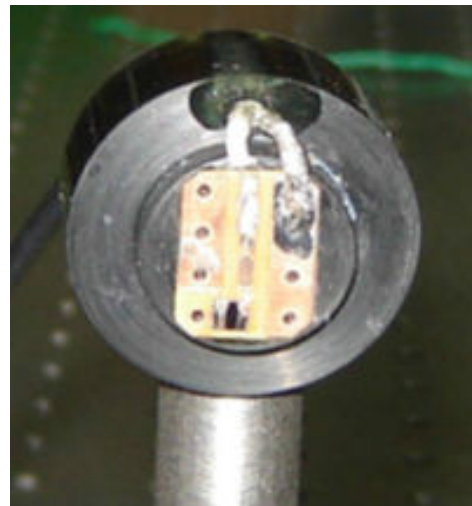


FIGURE 2. Photograph of the p-emf sensor employed.

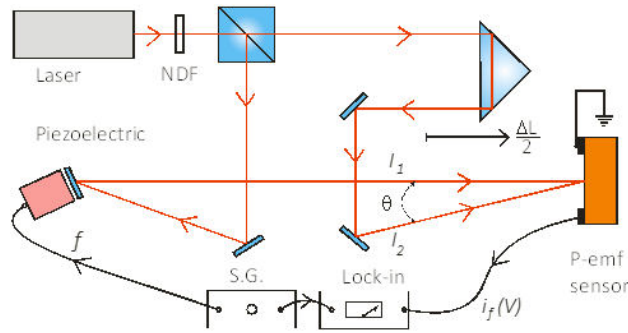


FIGURE 3. Experimental setup for measuring the coherence length of a He-Ne laser using a p-emf sensor. NDF: neutral density filter, S.G.: signal generator.

2. Experimental setup

A schematic diagram of the experimental setup for measuring the coherence length of a light source using a p-emf sensor is depicted in Fig. 3.

The light source used in the present experiment was a He-Ne laser. It has an output power of 10 mW and an emission wavelength of 632.8 nm. To avoid saturating the p-emf sensor, the output beam was attenuated with a neutral density filter of 0.3. The laser beam was not collimated. A nonpolarizing beam splitter divided the beam into two beams. The optical path of one of them, labelled beam 1, was kept constant, while the optical path of beam 2 was modified using a prism mounted on a translation stage. The beams interfere over the p-emf sensor at an angle of $\theta = 1/40$ rad.

The phase modulation –and the corresponding vibration of the interference pattern– was introduced in the beam 1. It was carried out by reflecting the beam 1 on a mirror attached to a piezoelectric transducer driven by a signal generator. The electrical current generated by the p-emf sensor, i_f (V), or p-emf signal, was measured as a voltage drop across the input impedance (≈ 100 M Ω , 25 pF) of the lock-in amplifier, which was referenced to the signal of the function generator. The p-emf signals were large enough to also be measured using an oscilloscope.

The optical table used for the experiment was not isolated from environmental perturbations. Additionally, the measurements were conducted with the laboratory lights on, and no optical bandpass filter was placed in front of the p-emf sensor.

Note that this experimental setup is a modification of the one presented in Ref. [11]. The setup in Ref. [11] was specifically designed to work with speckle patterns and small optical path differences (on the order of tens of microns). In contrast, the setup presented here uses Gaussian beams and allows for handling optical path differences of several tens of centimeters, making it possible to observe the revivals of the longitudinal coherence of a He-Ne laser.

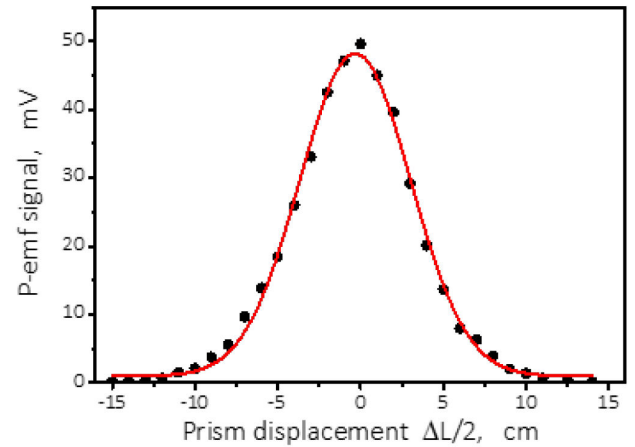


FIGURE 4. P-emf signal as a function of the prism displacement. The intensities of the interfering beams were $I_1 = 1.7$ mW and $I_2 = 1.55$ mW. The piezoelectric vibration frequency f was set at 610 Hz. The solid line is a Gaussian fit to the experimental data.

3. Experimental results and discussion

Figure 4 shows the dependence of the detected p-emf signal as a function of the prism displacement, with increments of 1.0 cm. Note that the prism displacement is equal to half of the optical path difference between the interfering beams, $\Delta L/2$.

The p-emf signal was found to be stable. Indeed, the fluctuations in the p-emf signal and the uncertainties in the prism displacement are smaller than the size of the data points used to indicate the mean values in Fig. 4.

The data presented in Fig. 4 can be re-plotted in a more conventional manner. By taking the square root of the p-emf values and normalizing them, we obtain the visibility of the interference pattern. These visibility values are then plotted in Fig. 5 as a function of the optical path difference, which corresponds to twice the prism displacement.

The processed experimental data fit well to a Gaussian dependence, with a coefficient of determination $R^2 \approx 0.99$. The visibility V (which is proportional to the square root of the p-emf signal) as a function of the optical path difference ΔL can be expressed as [14]:

$$V(\Delta L) = \exp\left(-\frac{4 \ln(2)(\Delta L)^2}{L_c^2}\right), \quad (5)$$

where L_c is the coherence length, which is defined as the Full Width at Half Maximum (FWHM) of this dependence. From the data, we determine $L_c = (22.5 \pm 0.4)$ cm, that is, a percentage uncertainty of 1.8% for the value of the coherence length of the employed laser. This value is consistent with the reported values for the coherence length of He-Ne lasers.

Note that the coherence length of the most commercial He-Ne lasers is typically reported to be 10 [5], 20 [15] and

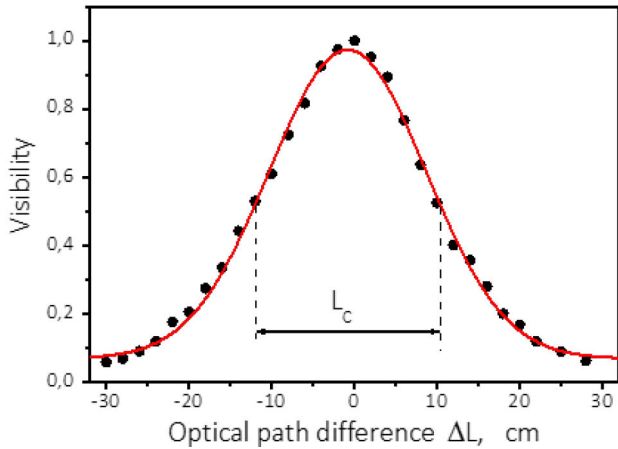


FIGURE 5. Square root of the p-emf signal as a function of the optical path difference. A Gaussian fit was applied to the experimental data (solid line).

25 cm [7]. However, this length can be modified by alterations of the Doppler line shape and oscillations of non-adjacent modes [16]. The reported percentage uncertainties in the physical parameters measured by different methods are around 5% [5,17], while the percentage uncertainties in the determined coherence lengths can be as low as 0.75% [18].

The temporal coherence of a He-Ne laser is a periodic property. It will replicate at optical path differences L_n given by:

$$L_n = n \cdot 2d, \quad (6)$$

where n is an integer number and d is the laser optical cavity length. The origin of these revivals is due to the beat frequency between the different longitudinal modes of the laser cavity that lie within the gain curve of the laser medium.

Figure 6 shows the p-emf signal as a function of the optical path difference over an extended range of measurements compared to those presented in Fig. 4.

From the experimental data, we obtained a separation between the peaks of (44 ± 0.1) cm. Using Eq. 6 for $n = 1$ this implies that the cavity length d is equal to this separation.

The cavity length of the laser is not specified directly; instead, the manufacturer states that the frequency spacing $\delta\nu$ between the longitudinal modes of the laser is $\delta\nu = 341$ MHz. Using the relationship between the frequency spacing and the laser length given by:

$$\delta\nu = \frac{c}{2d}, \quad (7)$$

we obtain a theoretical value of $d \cong 44$ cm, which agrees with the experimental result indicated above.

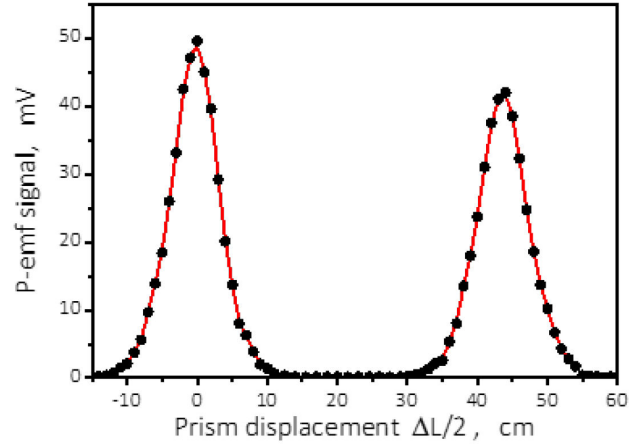


FIGURE 6. P-emf signal as a function of the prism displacement in an extended measurement range. The solid line is a b-spline to the data.

The maxima of the signal presented in Fig. 6 do not have the same value. This is due to the divergence of the laser beam, which, as mentioned earlier, is not collimated. Since the p-emf signal is proportional to the irradiance incident on it, larger beam spots result in a lower p-emf signal.

4. Conclusions

We have demonstrated the use of p-emf sensors to determine the coherence length of a light source. We illustrated our method by determining the coherence length of a He-Ne laser and the associated length corresponding to the beat frequency of the longitudinal modes of the laser cavity.

The gradual changes in the visibility of the interference pattern, as the optical path is varied, are easily detected and quantified by the electrical current generated by the p-emf sensors. Since the measurements are in real-time and do not require any signal processing, the proposed method in this work can be faster than the CCD-based methods. Because the p-emf signals present a high signal-to-noise ratio even if the interfering beams are spatially irregular or affected with speckle patterns and can suppress environmental perturbations, it is possible to carry out the experiment without the need for high-quality optical elements and vibration isolation optical tables. Additionally, in contrast to conventional methods, the one presented in this paper does not require stringent alignment. Therefore, the proposed method is suitable for implementation in a standard-equipped undergraduate laboratory.

The proposed method is simple, inexpensive, robust, and reliable. Using p-emf sensors fabricated from GaAs or CdTe crystals, it is possible to determine the coherence length of lasers emitting in the visible and near-infrared regions of the spectrum.

1. L.-P. Leppänen *et al.*, Measurement of the degree of temporal coherence of unpolarized light beams, *Photonics Res.* **5** (2017) 156, <https://doi.org/10.1364/PRJ.5.000156>
2. R. Dubey and R. Kumar, A simple setup for measurement of the coherence length of a laser diode using holographic optics, *Eur. J. Phys.* **40** (2019) 055304, <https://doi.org/10.1088/1361-6404/ab1d6a>
3. P. Pogany *et al.*, Measuring the coherence function of continuous-wave lasers by a photorefractive grating method, *Appl. Opt.* **38** (1999) 516, <https://doi.org/10.1364/AO.38.000516>
4. S. Alaruri, Experimental Method for Determining the Coherence Length of CW Lasers Using a Michelson Interferometer, *J. Laser Appl.* **5** (1993) 33, <https://doi.org/10.2351/1.4745328>
5. M. Illarramendi *et al.*, Adaption of the Michelson interferometer for a better understanding of the temporal coherence in lasers, In X. Liu and X.-C. Zhang, eds., 14th Conference on Education and Training in Optics and Photonics: ETOP 2017, vol. **10452**, *International Society for Optics and Photonics* (SPIE, 2017) p. 1045249, <https://doi.org/10.1117/12.2266546>
6. S. Stepanov, Chapter 6 - Photo-electromotive-force effect in semiconductors, In H. Singh Nalwa, ed., *Handbook of Advanced Electronic and Photonic Materials and Devices*, pp. 205-272 (Academic Press, Burlington, 2001), <https://doi.org/10.1016/B978-012513745-4/50026-3>.
7. E. Hecht, *Optics* 5th ed. (Pearson Education India, 2017), p. 601 and p. 628.
8. P. Rodriguez-Montero, C. M. Gómez-Sarabia, and J. Ojeda-Castaneda, Adaptive photodetector for assisted Talbot effect, *Appl. Opt.* **47** (2008) 3778, <https://doi.org/10.1364/AO.47.003778>
9. P. R. Montero, Observation and verification of the Fresnel and Arago interference laws using adaptive photodetectors, *Rev. Mex. Fis. E* **18** (2021) 44, <https://doi.org/10.31349/RevMexFisE.18.44>
10. S. Stepanov *et al.*, Effective broadband detection of nanometer laser-induced ultrasonic surface displacements by CdTe: V adaptive photoelectromotive force detector, *Appl. Phys. Lett.* **84** (2004) 446, <https://doi.org/10.1063/1.1640466>
11. M. A. Carrasco, P. R. Montero, and S. Stepanov, Measurement of the coherence length of diffusely scattered laser beams with adaptive photodetectors, *Opt. Commun.* **157** (1998) 105, [https://doi.org/10.1016/S0030-4018\(98\)00537-9](https://doi.org/10.1016/S0030-4018(98)00537-9)
12. Y. Ding *et al.*, Electric-field correlation of femtosecond pulses by use of a photoelectromotive-force detector, *JOSA B* **15** (1998) 2013, <https://doi.org/10.1364/JOSAB.15.002013>
13. C.-C. Wang *et al.*, Human life signs detection using high-sensitivity pulsed laser vibrometer, *IEEE Sens. J.* **7** (2007) 1370, <https://doi.org/10.1109/JSEN.2007.905041>
14. Y. Pan *et al.*, Low-coherence optical tomography in turbid tissue: theoretical analysis, *Appl. Opt.* **34** (1995) 6564, <https://doi.org/10.1364/AO.34.006564>
15. B. E. Saleh and M. C. Teich, *Fundamentals of photonics* (John Wiley & Sons, Ltd, 1991), p. 532, <https://doi.org/10.1002/0471213748.fmatterindsub>
16. E. F. Erickson and R. M. Brown, Calculation of fringe visibility in a laser-illuminated interferometer, *JOSA* **57** (1967) 367, <https://doi.org/10.1364/JOSA.57.000367>
17. M. K. Singh and S. Datta, Dual measurements of temporal and spatial coherence of light in a single experimental setup using a modified Michelson interferometer, *Rev. Sci. Instrum.* **92** (2021) 105109, <https://doi.org/10.1063/5.0041438>
18. K. Pieper *et al.*, Visualizing and manipulating the spatial and temporal coherence of light with an adjustable light source in an undergraduate experiment, *Eur. J. Phys.* **40** (2019) 055302, <https://doi.org/10.1088/1361-6404/ab3035>